Electrochimica Acta 55 (2010) 5014–5018

Contents lists available at ScienceDirect

Electrochimica Acta

journal homepage: www.elsevier.com/locate/electacta

A feasible kinetic model for the hydrogen oxidation on ruthenium electrodes

M.S. Rau, M.R. Gennero de Chialvo, A.C. Chialvo *,[1]

Programa de Electroquímica Aplicada e Ingeniería Electroquímica (PRELINE), Facultad de Ingeniería Química, Universidad Nacional del Litoral, Santiago del Estero 2829, 3000 Santa Fe, Argentina

ARTICLE INFO

Article history:
Received 1 March 2010
Received in revised form 30 March 2010
Accepted 3 April 2010
Available online 13 April 2010

Keywords:
Hydrogen oxidation
Ruthenium
Kinetic parameters
Electrocatalytic activity

ABSTRACT

The hydrogen oxidation reaction (*hor*) was studied on a polycrystalline ruthenium electrode in H_2SO_4 solution at different rotation rates (ω). The experimental polarization curves recorded on steady state show the existence of a maximum current with a non-linear dependence of the current density on $\omega^{1/2}$. On the basis of the Tafel–Heyrovsky–Volmer kinetic mechanism, coupled with a process of inhibition of active sites by the reversible electroadsorption of hydroxyl species, it was possible to appropriately describe the origin of the maximum current. The corresponding set of kinetic parameters was also calculated from the correlation of the experimental results with the proposed kinetic model.

1. Introduction

Studies of the hydrogen electrode reaction on ruthenium electrodes are scarce and they have been carried out preferably in the cathodic overpotentials range, which corresponds to the hydrogen evolution reaction (*her*) [1–4]. The hydrogen oxidation reaction (*hor*), less studied, was evaluated on rotating disc electrodes of polycrystalline [5] as well as single crystal ruthenium [6]. It was also studied by a.c. impedance at the open circuit potential on a Ru/C electrode [7]. The important results obtained for the *hor* on a polycrystalline Ru electrode by Gasteiger et al. show a more complex behaviour than that observed on platinum in similar experimental conditions [5]. This behaviour is characterized by the presence of a peak in the current density (j)–overpotential (η) curves. These curves display a diffusion contribution, as it can be appreciated by the increase of the current density with the increase of the rotation rate (Fig. 2 in Ref. [5] and Fig. 3 in Ref. [6]). However, the current values at a given overpotential do not vary linearly with the square root of the rotation rate (the Levich equation). Taking into account that ruthenium is recognized by its high oxyphilic properties, these authors concluded that the current density decrease is due to the inhibition of the adsorption of the reaction intermediate H_{ad} due to the presence of OH_{ad} species on the electrode surface [5]. Then, Inoue et al., studying the *hor* on Ru (0 0 0 1) and (1 0 1 0) single crystal surfaces, found that simple blocking effect of RuOH was not sufficient to explain the observed kinetics, although they did not give any further explanations [6].

The ability of Ru to oxidise CO is based precisely on the presence of OH_{ad} on the electrode surface, being the reaction between CO_{ad} and OH_{ad} one of the steps of the most accepted reaction mechanism of the carbon monoxide oxidation reaction [8–10]. Furthermore, as OH_{ad} species are intrinsically related to the interaction between Ru and the electrolyte solution [11] in the overpotentials range corresponding to the *hor*, they should be included in the kinetic analysis of the hydrogen electrooxidation.

In this context, the present work intends to verify if the unusual experimental current–overpotential dependence in steady state for the *hor* on a smooth polycrystalline ruthenium electrode can be interpreted through the Tafel–Heyrovsky–Volmer kinetic mechanism coupled with the adsorption process of oxygen-containing species.

2. Experimental

Measurements were carried out in a three electrodes cell specially built for the use of a rotating electrode and with a particular design of the hydrogen saturator. The working electrode was a rotating disc of polycrystalline ruthenium (MaTecK GmbH) with a geometric area of 0.07 cm^2. The rotation rate was varied in the range $900 \leq \omega\ (\text{rpm}) \leq 4900$ through the use of a rotating disc Radiometer EDI 10K. The counterelectrode was a platinum helical wire of large area. The electrolytic solution was 0.5 M H_2SO_4, prepared with ultra-pure water (PureLab, Elga LabWater). Measurements were carried out at 30 °C under hydrogen gas bubbling at 1 bar, ensuring a continuous saturation of the electrolyte with molecular hydro-

* Corresponding author. Tel.: +54 342 457 1164x2519; fax: +54 342 453 6861.
E-mail address: achialvo@fiq.unl.edu.ar (A.C. Chialvo).
[1] ISE member.

0013-4686/$ – see front matter © 2010 Elsevier Ltd. All rights reserved.
doi:10.1016/j.electacta.2010.04.007

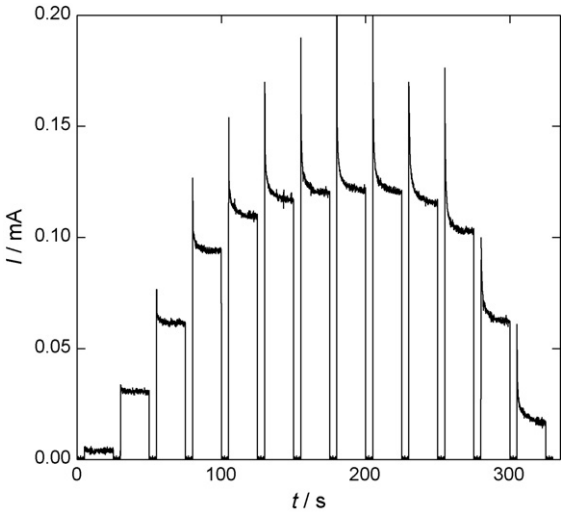

Fig. 1. Current vs. time response to a potential program applied to a polycrystalline Ru electrode rotated at 900 rpm. 0.5 M H_2SO_4, 30 °C.

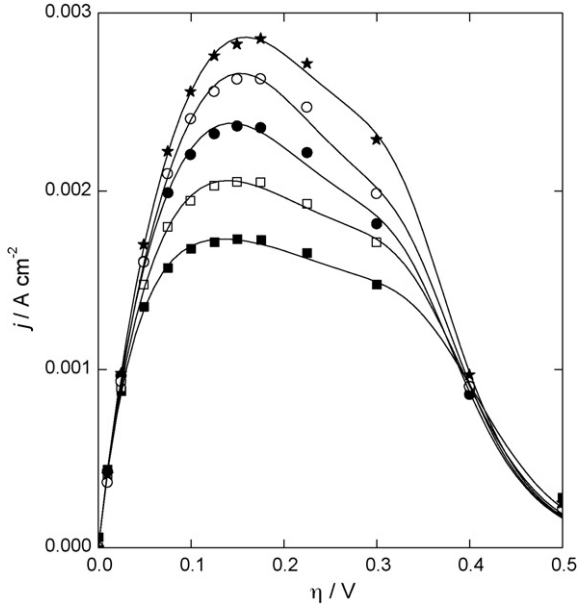

Fig. 2. Experimental (symbols) and simulated (lines) $j(\eta)$ curves of the *hor* on polycrystalline Ru in the range $0.0 \leq \eta\,(V) \leq 0.5$. 0.5 M H_2SO_4, 30 °C. ω= (■) 900; (□) 1600; (●) 2500; (○) 3600; (⋆) 4900 rpm. Kinetic parameters from Table 1.

gen. The applied overpotentials ($0.0 \leq \eta\,(V) \leq 0.5$) were controlled with respect to a reversible hydrogen electrode in the same solution (RHE) and therefore potentials (E) are coincident with overpotentials (η).

For the determination of the experimental current–overpotential dependences $j_{exp}(\eta,\omega)$, the working electrode was mechanically polished with emery paper 1200 grit, followed by sonication in ultra-pure water for 5 min. In these conditions, it was subjected to cyclic voltammetry between 0.0 and 1.3 V (vs. RHE) at 0.1 V s^{-1} in the electrolyte solution saturated with nitrogen gas and the stabilized potentiodynamic profile was recorded. Then the electric circuit was opened and simultaneously the nitrogen bubbling was replaced by hydrogen. The open circuit potential decreases from an initial value of 0.5 V to 0.0 ± 0.0005 V, achieving the equilibrium potential of the hydrogen electrode. Starting from these conditions a potential program was applied, initiated with 5 s at 0.0 V, followed by a step to the desired overpotential value, which was maintained during 20 s. In this period, readings of the current value were made each 0.1 s. In order to ensure that the steady state current was reached, the mean value of the current data measured in the last 5 s was assigned to the step overpotential. Then the electrode was returned to the equilibrium potential and the program was repeated for each η value and thus the experimental curve $j(\eta)$ for $0.0 \leq \eta\,(V) \leq 0.5$ and a given rotation rate was built. In order to ensure the quality of the measurements, special attention was paid to the solution purity and the efficient saturation of the solution with molecular hydrogen.

3. Results

3.1. Current density–overpotential curves

The current (I)–time (t) response of the polycrystalline Ru electrode resulting from the application of the potential program described above is shown in Fig. 1, for the case corresponding to a rotation rate of 900 rpm. Similar plots were obtained for the other rotation rates (1600, 2500, 3600 and 4900 rpm). Starting from these results, the corresponding $j(\eta)$ dependences on steady state were evaluated, which are shown in Fig. 2 (symbols). These results are similar to those previously obtained through the use of potentiodynamic sweeps [5,6] and they are characterized by the existence of a current peak at $\eta \cong 0.15$ V. Two important aspects emerge from the analysis of these curves. One is that the peak current values do not vary linearly with the square root of the rotation rate ($\omega^{1/2}$), as it can be observed in Fig. 3. This result is in agreement with that reported in Ref. [6] and denotes a substantial difference with the behaviour of platinum, where a well-defined current plateau with a linear variation on $\omega^{1/2}$ is obtained [12–16]. The second aspect is that the limiting diffusion current density (j_L) is not reached at any value of the rotation rate. It can be calculated by the Levich equation $j_L = B\omega^{1/2}$ [17], where the parameter B depends on temperature and on the electrolyte solution. The value $B = 6.88 \times 10^{-5}$ A cm^{-2} $rpm^{-1/2}$ was used, which was experimentally obtained in previous studies for the same electrode configuration, temperature and electrolyte solution [13]. The resulting values were included in Fig. 3, where it can be observed the difference between j_L and the peak current density at each rotation rate.

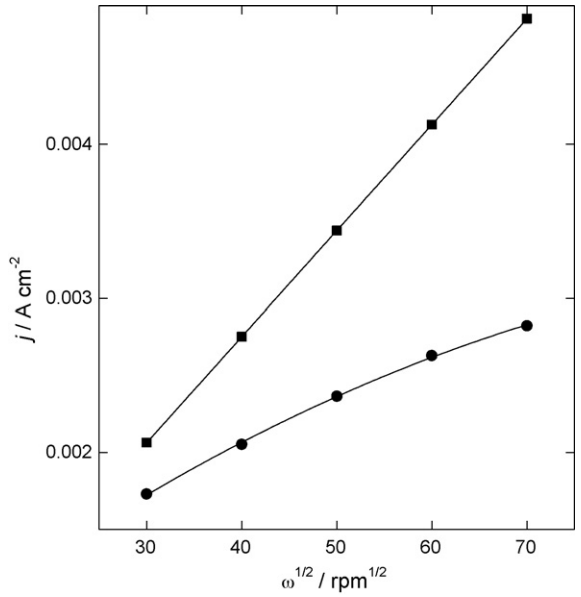

Fig. 3. Current density vs. $\omega^{1/2}$ plot. (●) at $\eta = 0.15$ V; (■) j_L.

Table 1
Kinetic parameters of the *hor* on Ru electrode at different rotation rates obtained from the correlation of the experimental $j(\eta)$ curves.

Kinetic parameters	Rotation rate (rpm)					SD
	900	1600	2500	3600	4900	
ν_T^e (mol cm^{-2} s^{-1})	4.87×10^{-9}	4.60×10^{-9}	5.36×10^{-9}	6.22×10^{-9}	6.40×10^{-9}	7.15×10^{-10}
ν_H^e (mol cm^{-2} s^{-1})	3.58×10^{-7}	1.26×10^{-7}	5.35×10^{-8}	3.08×10^{-8}	3.16×10^{-8}	1.24×10^{-7}
ν_V^e (mol cm^{-2} s^{-1})	2.37×10^{-11}	2.86×10^{-11}	3.05×10^{-11}	3.10×10^{-11}	4.16×10^{-11}	5.86×10^{-12}
θ_H	0.580	0.581	0.580	0.581	0.585	1.85×10^{-3}
θ_{OH}	0.0166	0.0072	0.0035	0.0020	0.0020	5.51×10^{-3}

3.2. Mechanistic description of the hydrogen oxidation on Ru

It is well known that the hydrogen electrode reaction on a metallic surface is verified through the elementary steps of Tafel, Heyrovsky and Volmer,

$$H_2 + 2S \rightleftarrows 2H_{ad} \quad \text{Tafel} \tag{1}$$

$$H_2 + S \rightleftarrows H_{ad} + H^+ + e^- \quad \text{Heyrovsky} \tag{2}$$

$$H_{ad} \rightleftarrows H^+ + e^- + S \quad \text{Volmer} \tag{3}$$

where S represents a site on the electrode surface in which the reaction intermediate H_{ad} can be adsorbed. On the other hand, it is known that in the overpotentials range where the hydrogen oxidation is verified on Ru electrodes, there are also OH_{ad} species on the electrode surface originated in the following reaction [5–11]:

$$S + H_2O \rightleftarrows OH_{ad} + H^+ + e^- \tag{4}$$

It is considered in Eq. (4) that the surface sites where OH_{ad} is adsorbed are of the same type of those where the adsorption of H_{ad} takes place. Consequently, reactions ((1)–(3)) are the steps of the kinetic mechanism of the hydrogen oxidation on ruthenium electrodes, while reaction (4) inhibits surface sites needed for the adsorption of the reaction intermediate of the *hor*. In this sense it should be noticed that when the *hor* reaches the steady state at a given overpotential, reaction (4) is at an equilibrium state corresponding to such η value. This is due to that OH_{ad} does not participate in the formation of protons and therefore when the potential and the diffusion layer thickness are fixed, the steady state imposes the equilibrium condition for reaction (4).

3.3. Derivation of the kinetic expressions

The derivation of the theoretical expressions for the $j(\eta)$ dependence on steady state will be carried out following the procedure previously developed [12–14]. The main difference is that in this case the surface coverage (θ) is the sum of two contributions, the hydrogen coverage (θ_H) and the hydroxyl coverage (θ_{OH}), respectively,

$$\theta = \theta_H + \theta_{OH} \tag{5}$$

From the resolution of the Tafel–Heyrovsky–Volmer kinetic mechanism on steady state, taking into account the diffusion contribution and considering a Langmuir type adsorption of the reaction intermediate H_{ad}, the following expressions are obtained:

$$j = \frac{\nu_V^e[\theta_H e^{\alpha f\eta}/\theta_H^e - (1-\theta)e^{(\alpha-1)f\eta}/(1-\theta^e)] + \nu_H^e[(1-\theta)e^{\alpha f\eta}/(1-\theta^e) - \theta_H e^{(\alpha-1)f\eta}/\theta_H^e]}{[1/F + \nu_H^e(1-\theta)e^{\alpha f\eta}/(1-\theta^e)j_L]} \tag{6}$$

$$j = \frac{\nu_T^e[(1-\theta)^2/(1-\theta^e)^2 - \theta_H^2/\theta_H^{e2}] + \nu_H^e[(1-\theta)e^{\alpha f\eta}/(1-\theta^e) - \theta_H e^{(\alpha-1)f\eta}/\theta_H^e]}{[1/2F + \nu_H^e(1-\theta)e^{\alpha f\eta}/(1-\theta^e)j_L + \nu_T^e(1-\theta)^2/(1-\theta^e)^2 j_L]} \tag{7}$$

$$j = \frac{\nu_V^e[\theta_H e^{\alpha f\eta}/\theta_H^e - (1-\theta)e^{(\alpha-1)f\eta}/(1-\theta^e)] - \nu_T^e[(1-\theta)^2/(1-\theta^e)^2 - \theta_H^2/\theta_H^{e2}]}{[1/2F - \nu_T^e(1-\theta)^2/(1-\theta^e)^2 j_L]} \tag{8}$$

where ν_i^e (i = T, H, V) is the equilibrium reaction rate of the elementary step i, α is the symmetry factor of the step i, considered equal for the Heyrovsky and Volmer steps ($\alpha_V = \alpha_H = \alpha$), j_L is the limiting diffusion current density, $f = F/RT$ and the superscript e indicates the equilibrium condition for the hydrogen oxidation ($\eta = 0$). On the other hand, the dependence $\theta_{OH}(\eta)$ can be obtained from the application of the equilibrium condition to reaction (4) that is accomplished for a given value of η at which the hydrogen oxidation is on steady state. The corresponding expression (see Appendix A) is

$$\theta_{OH} = \frac{\theta_{OH}^e(1-\theta_H)e^{f\eta}}{1-\theta^e+\theta_{OH}^e e^{f\eta}} \tag{9}$$

being θ_{OH}^e the OH_{ad} coverage at $\eta = 0$. Operating with two of the expressions of $j(\eta)$, e.g. Eqs. (6) and (7), together with Eq. (9), an implicit expression for the dependence $\theta_H(\eta)$ is obtained:

$$\left\{\nu_V^e\left[\frac{\theta_H e^{\alpha f\eta}}{\theta_H^e} - \frac{(1-\theta)e^{(\alpha-1)f\eta}}{(1-\theta^e)}\right] + \nu_H^e\left[\frac{(1-\theta)e^{\alpha f\eta}}{(1-\theta^e)} - \frac{\theta_H e^{(\alpha-1)f\eta}}{\theta_H^e}\right]\right\} \times \left[\frac{1}{2F} + \frac{\nu_H^e(1-\theta)e^{\alpha f\eta}}{(1-\theta^e)j_L} + \frac{\nu_T^e(1-\theta)^2}{(1-\theta^e)^2 j_L}\right] - \left[\frac{1}{F} + \frac{\nu_H^e(1-\theta)e^{\alpha f\eta}}{(1-\theta^e)j_L}\right] \times \left\{\nu_T^e\left[\frac{(1-\theta)^2}{(1-\theta^e)^2} - \frac{\theta_H^2}{\theta_H^{e2}}\right] + \nu_H^e\left[\frac{(1-\theta)e^{\alpha f\eta}}{(1-\theta^e)} - \frac{\theta_H e^{(\alpha-1)f\eta}}{\theta_H^e}\right]\right\} = 0 \tag{10}$$

With Eq. (10), the description of the kinetics of the hydrogen oxidation on a ruthenium electrode is completed.

3.4. Fitting capability of the proposed kinetic model

Through the use of one of the Eqs. (6)–(8) and (10), the experimental dependence $j(\eta)$ on steady state for each values of the rotation rate ($900 \le \omega\,(\text{rpm}) \le 4900$) was correlated and the corresponding set of kinetic parameters was evaluated. The parameters obtained by non-linear least squares regression of the experimental results were ν_T^e, ν_H^e, ν_V^e, θ_H^e and θ_{OH}^e. The symmetry factor α was fixed to 0.5.

Table 1 shows the values of the kinetic parameters evaluated through the correlation of the experimental curves depicted in Fig. 2 (symbols). The values of the standard deviation (SD) are given in the last column of Table 1, evaluated from the five values of each parameter obtained for the different rotation rates. The corresponding simulations of these dependencies are shown in Fig. 2 as continuous lines. It can be observed that the agreement between the experimental and fitted curves is very good for all the values of the rotation rate. Therefore, the inhibition

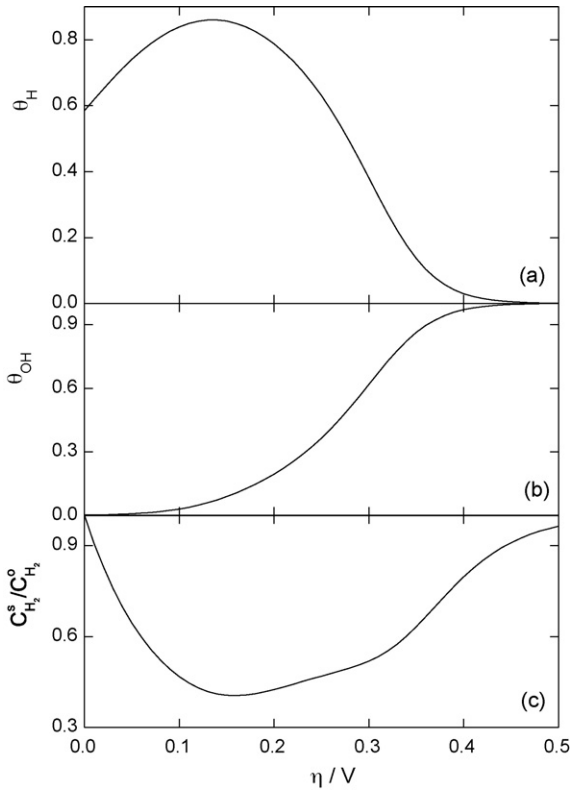

Fig. 4. Simulated dependences of the *hor* at $\omega = 4900$ rpm: (a) θ_H vs. η; (b) θ_{OH} vs. η; (c) $C^s_{H_2}/C^o_{H_2}$ vs. η. Kinetic parameters from Table 1.

effect on the reaction rate of the hydrogen oxidation on a ruthenium electrode due to the reversible adsorption of hydroxyl species can satisfactorily explain the experimental behaviour.

3.5. Dependence of θ_H, θ_{OH} and $C^s_{H_2}/C^o_{H_2}$ on overpotential

A direct consequence of the theoretical expressions (Eqs. (6)–(10)) derived from the resolution of the kinetic mechanism is the possibility of indirectly know the dependence on overpotential of the surface coverage of the reaction intermediate $\theta_H(\eta)$, that of the inhibitor $\theta_{OH}(\eta)$ as well as the relationship between the concentration of molecular hydrogen on the reaction plane and in the bulk, respectively ($C^s_{H_2}(\eta)/C^o_{H_2}$). The hydrogen coverage $\theta_H(\eta)$ is evaluated from Eq. (10) and then $\theta_{OH}(\eta)$ is evaluated from Eq. (9). Otherwise, the molecular hydrogen concentration relationship can be calculated from $C^s_{H_2}/C^o_{H_2} = 1 - [j(\eta)/j_L]$, using one of the Eqs. (6)–(8) and the parameters given in Table 1. In order to illustrate these dependences, Fig. 4(a–c) shows the corresponding curves for $\omega = 4900$ rpm in the range $0.0 \le \eta\,(V) \le 0.5$. It can be observed that at low overpotentials both coverages, θ_H (Fig. 4a) and θ_{OH} (Fig. 4b), increase. Meanwhile the surface concentration of molecular hydrogen (Fig. 4c) decreases at low η. The coverage of the reaction intermediate θ_H reaches a maximum value near $\eta = 0.13$ V, whereas that of OH_{ad} presents an inflection point near $\eta = 0.3$ V and the relationship $C^s_{H_2}/C^o_{H_2}$ reaches its minimum value at $\eta \cong 0.15$ V. The inhibitor coverage exhibits a strong increase, achieving at $\eta \cong 0.45$ V a value near unity ($\theta_{OH} \cong 1$). Consequently, as all the active sites for the hydrogen oxidation are inhibited, the hydrogen coverage vanishes, as well as the current density. This means that the reaction rate of the Tafel step also vanishes ($v_T \to 0$).

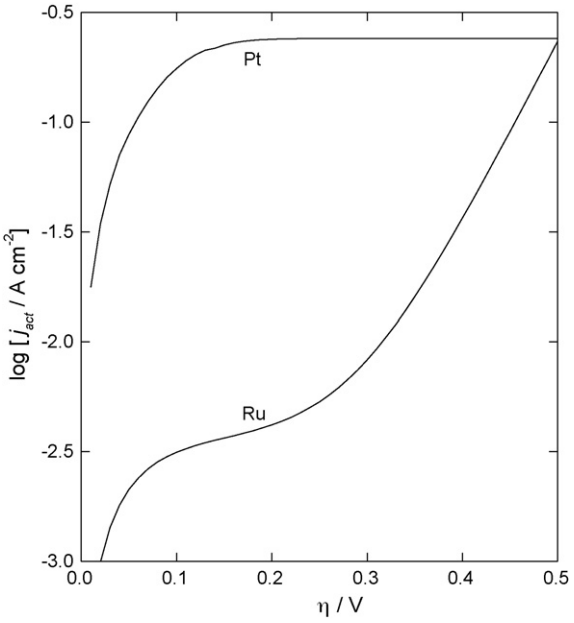

Fig. 5. Simulation of $\log j_{act}$ vs. η curves for Ru and Pt electrodes. Kinetic parameters from Table 1 (Ru) and Ref. [11] (Pt).

3.6. Electrocatalytic activity of Ru vs. Pt

In order to compare the electrocatalytic activity of the Ru electrode with that of Pt, the dependence of the logarithm of the activated current density on overpotential was simulated for both metals in the same kinetic conditions, in absence of diffusion contribution ($j_L \to \infty$) and for the case of Ru also in absence of the inhibition process due to the adsorbed hydroxyl ($\theta^e_{OH} = 0$). The kinetic parameters for the simulation of the $\log j_{act}$ vs. η on Pt were taken from a previous work, with conditions similar to the present case [11]. They were: $v^e_T = 1.25 \times 10^{-6}$ mol cm^{-2} s^{-1}, $v^e_H = 1.0 \times 10^{-14}$ mol cm^{-2} s^{-1}, $v^e_V = 5.25 \times 10^{-7}$ mol cm^{-2} s^{-1} and $\theta^e_H = 1.0 \times 10^{-7}$. The results obtained are illustrated in Fig. 5, where it can be clearly appreciated that the electrocatalytic activity of the ruthenium electrode for the *hor* is significantly lower than that of platinum. The difference is almost two orders of magnitude for $\eta < 0.3$ V. This result is in agreement with others obtained voltammetrically [5,6].

4. Discussion

The hydrogen oxidation reaction has been mainly studied on Pt electrodes, where the increase in overpotential leads to a plateau in the dependence $j(\eta)$ at a given rotation rate [12–16]. In conditions of high mass transfer rate [18,19], this plateau can be preceded by a shoulder indicating a transition from the Tafel–Volmer route at low overpotentials to the Heyrovsky-Volmer route at high η values [19,20]. This behaviour is different to that observed on a polycrystalline Ru electrode, where the hydrogen oxidation takes place in a more complex way, manifested through the definition of a maximum in the dependence $j(\eta)$ at any rotation rate. The origin of this behaviour is attributed to the reversible inhibition of the adsorption sites of the reaction intermediate by OH species. The adsorption of such species in the overpotentials range of the *hor*, which was already detected by spectroscopic techniques [21], was taken into account in the proposed kinetic model. Otherwise, the OH adsorption can also be observed on Pt electrodes, but only at $\eta > 0.60$ V [22,23]. It can explain the decrease of the current density for the *hor* on this metal at very high overpotentials [24,25]. Consequently, the

assumption that OH is adsorbed on the same active sites than those that can be occupied by the reaction intermediate H_{ad} is reasonable and allows to interpret the hydrogen oxidation on Ru.

The behaviour of the hydrogen oxidation on Ru electrodes was studied previously [5,6] through the use of potentiodynamic sweeps at relatively high sweep rates (20 mV s^{-1}). In these experimental runs, the resulting $j(\eta)$ plot show a pronounce hysteresis between the profiles corresponding to the anodic and cathodic sweep (see Fig. 2 in Ref. [5]), originated in the non-steady state conditions. The pseudocapacitive processes related to the adsorption of H_{ad} and OH_{ad} possibly explain the slight differences in the shape of the current peaks with respect to that of the present results. The current densities are also different, being lower in this work, as it can be expected when potentiodynamic and steady state responses are compared. Nevertheless, such previous studies [5,6] provided the first results known of the *hor* on Ru, highlighting the existence of an unusual behaviour characterized by the presence of a peak in the $j(\eta)$ plot and stating that OH adsorption is an important process in the reaction kinetics, although the authors concluded that this process alone cannot describe the abrupt decline of the current density [6]. Moreover, the present study has demonstrated that the experimental behaviour of the *hor* on polycrystalline Ru electrodes on steady state can be properly interpreted through the Tafel–Heyrovsky–Volmer kinetic mechanism together with the reversible electroadsorption of OH species.

Finally, it is important to compare the behaviour of Ru and Pt electrodes for the hydrogen oxidation reaction. It can be observed from the comparison of the kinetic parameters that there is a marked difference in the corresponding contribution of each elementary step to the reaction mechanism. It can be appreciated that $\nu^{e}_{H(Ru)} > \nu^{e}_{H(Pt)}$, $\nu^{e}_{V(Ru)} < \nu^{e}_{V(Pt)}$ and $\nu^{e}_{T(Ru)} < \nu^{e}_{T(Pt)}$, which show that for Ru electrodes the Heyrovsky step is more important than that of Tafel, leading to a marked difference between the behaviour of both metals towards the hydrogen oxidation (Fig. 5). These results are in agreement with the proposal made by Giorgi et al. [7], although their study was restricted to the open circuit potential.

5. Conclusions

The present work demonstrated that the Tafel–Heyrovsky–Volmer kinetic mechanism, coupled with a process of inhibition of active sites by the reversible electroadsorption of OH species, can describe adequately the experimental dependences of the current density on overpotential of the hydrogen oxidation reaction recorded at different rotation rates on a polycrystalline ruthenium electrode in H_2SO_4 solution. The proposed model allowed also for the first time the evaluation of a set of kinetic parameters from the correlation of the experimental results.

Acknowledgements

The authors wish to acknowledge the financial support received from ANPCyT, CONICET and UNL.

Appendix A. Derivation of Eq. (9)

The rate of reaction (4) is given by the following expression:

$$\nu_4 = k_{+OH} a_{H_2O} (1-\theta) e^{\alpha f E} - k_{-OH} a^{o}_{H^+} \theta_{OH} e^{(\alpha-1) f E} \quad (A.1)$$

where k_{+OH} and k_{-OH} are the specific constants of the forward and backward reaction rate, respectively, a_{H_2O} and $a^{o}_{H^+}$ are the activity of water and proton, respectively, α is the symmetry factor of the reaction and E is the electrode potential (vs. RHE). Applying the equilibrium condition,

$$k_{+OH} a_{H_2O} (1-\theta) e^{\alpha f E} = k_{-OH} a^{o}_{H^+} \theta_{OH} e^{(\alpha-1) f E} \quad (A.2)$$

In order to eliminate k_{+OH} and k_{-OH} and introduce the overpotential of the hydrogen oxidation reaction, Eq. (A.2) is rewritten for the particular case of the reversible hydrogen potential E^{e},

$$k_{+OH} a_{H_2O} (1-\theta^{e}) e^{\alpha f E^{e}} = k_{-OH} a^{o}_{H^+} \theta^{e}_{OH} e^{(\alpha-1) f E^{e}} \quad (A.3)$$

From the ratio of Eqs. (A.2) and (A.3), the following equation is obtained:

$$\frac{(1-\theta)}{(1-\theta^{e})} = \frac{\theta_{OH}}{\theta^{e}_{OH}} e^{-f(E-E^{e})} \quad (A.4)$$

Taking into account that $E - E^{e} = \eta$, substituting Eq. (5) into Eq. (A.4) and reordering, Eq. (9) is obtained.

References

[1] R.D. Giles, J.A. Harrison, H.R. Thirsk, J. Electroanal. Chem. 20 (1969) 47.
[2] A.T. Kuhn, P.M. Wright, J. Electroanal. Chem. 27 (1970) 319.
[3] V.S. Bagotsky, A.M. Skundin, E.K. Tuseeva, Electrochim. Acta 21 (1976) 29.
[4] M.K. Breiter, J. Electroanal. Chem. 178 (1984) 53.
[5] H.A. Gasteiger, N.M. Markovic, P.N. Ross Jr., J. Phys. Chem. 99 (1995) 8290.
[6] H. Inoue, J.W. Wang, K. Sasaki, R.R. Adzic, J. Electroanal. Chem. 554–555 (2003) 77.
[7] L. Giorgi, A. Pozio, C. Bracchini, R. Giorgi, S. Turtu, J. Appl. Electrochem. 31 (2001) 325.
[8] F. Maillard, G.Q. Lu, A. Wieckowski, U. Stimming, J. Phys. Chem. B 109 (2005) 16230.
[9] T. Iwasita, H. Hoster, A. John-Anacker, W.F. Lin, W. Vielstich, Langmuir 16 (2000) 522.
[10] B. Andreaus, F. Maillard, J. Kocylo, E.R. Savinova, M. Eikerling, J. Phys. Chem. B 110 (2006) 21028.
[11] N.S. Marinkovic, M.B. Vukmirovic, R.R. Adzic, in: C.G. Vayenas, R.E. White, M.E. Gamboa-Aldeco (Eds.), Modern Aspects of Electrochemistry, vol. 42, Springer, New York, 2008 (Chapter 1).
[12] M.R. Gennero de Chialvo, A.C. Chialvo, Phys. Chem. Chem. Phys. 6 (2004) 4009.
[13] P.M. Quaino, M.R. Gennero de Chialvo, A.C. Chialvo, Phys. Chem. Chem. Phys. 6 (2004) 4450.
[14] M.R. Gennero de Chialvo, A.C. Chialvo, Curr. Top. Electrochem. 11 (2006) 1.
[15] N.M. Markovic, B.N. Grgur, P.N. Ross, J. Phys. Chem. B 101 (1997) 5405.
[16] A.F. Innocente, A.C.D. Angelo, J. Power Sources 162 (2006) 151.
[17] E. Gileadi, Electrode Kinetics for Chemistry, Chemical Engineering and Material Sciences, VCH, 1993, p. 87.
[18] S.L. Chen, A. Kucernak, J. Phys. Chem. B 108 (2004) 13984.
[19] M.A. Montero, M.R. Gennero de Chialvo, A.C. Chialvo, Electrochem. Commun. 12 (2010) 398.
[20] P.M. Quaino, J.L. Fernandez, M.R. Gennero de Chialvo, A.C. Chialvo, J. Mol. Catal. A: Chem. 252 (2006) 156.
[21] N.S. Marinkovic, J.X. Wang, H. Zajonz, R.R. Adzic, J. Electroanal. Chem. 500 (2001) 388.
[22] V. Climent, R. Gomez, J.M. Orts, J.M. Feliu, J. Phys. Chem. B 110 (2006) 11344.
[23] A. Berná, V. Climent, J.M. Feliu, Electrochem. Commun. 9 (2007) 2789.
[24] V.S. Bagotzky, N.V. Osetrova, J. Electroanal. Chem. 43 (1973) 233.
[25] Yu.M. Maksimov, B.J. Podlovchenko, Russ. J. Electrochem. 45 (2009) 1327.